Influence of rotor geometry on tip leakage and port flow areas in gerotor-type screw compressors

Journal:	*Part E: Journal of Process Mechanical Engineering*
Manuscript ID	JPME-19-0293.R1
Manuscript Type:	Special Issue Article
Date Submitted by the Author:	n/a
Complete List of Authors:	Read, Matthew; City University, Mechanical Engineering and Aeronautics Smith, I; City University, Mechanical Engineering and Aeronautics Stosic, Nikola; City University, Mechanical Engineering and Aeronautics
Keywords:	compressor, screw, gerotor, profiling, geometry, port
Abstract:	Conventional twin-screw compressors are positive displacement machines that form working chambers between two helical, parallel rotors and an outer casing. This study investigates an alternative configuration of rotors for compressor applications, in which the working chambers are formed by contact between and inner and outer rotors. This is a gerotor-type machine, which are commonly used in fuel and oil pumping applications and as hydraulic motors. For compressor applications, the use of helical rotors with appropriate porting in a gerotor-type compressor has been identified as having potentially lower rotor contact forces and larger port areas than occur with non-helical rotors. This study investigates how key performance parameters of a gerotor-type screw compressor (volume, port flow areas and tip leakage areas) are influenced by the profile, dimensions and wrap angle of the rotors. The results of this geometric analysis are compared with a conventional twin-screw machine, and suggest that the gerotor-type screw compressor can achieve higher axial port areas and lower tip leakage area over most of the compression cycle.

Influence of rotor geometry on tip leakage and port flow areas in gerotor-type twin screw compressors

M G Read*, I K Smith, N Stosic
City, University of London, Northampton Square, EC1V 0HB
E-mail: *corresponding author; m.read@city.ac.uk

Abstract. Conventional twin-screw compressors are positive displacement machines that form working chambers between two helical, parallel rotors and an outer casing. This study investigates an alternative configuration of rotors for compressor applications, in which the working chambers are formed by contact between and inner and outer rotors. This is a gerotor-type machine, which are commonly used in fuel and oil pumping applications and as hydraulic motors. For compressor applications, the use of helical rotors with appropriate porting in a gerotor-type compressor has been identified as having potentially lower rotor contact forces and larger port areas than occur with non-helical rotors. This study investigates how key performance parameters of a gerotor-type screw compressor (volume, port flow areas and tip leakage areas) are influenced by the profile, dimensions and wrap angle of the rotors. The results of this geometric analysis are compared with a conventional twin-screw machine, and suggest that the gerotor-type screw compressor can achieve higher axial port areas and lower tip leakage area over most of the compression cycle.

Keywords: compressor, screw, gerotor, geometry, port, leakage

1. Introduction

A gerotor pump consists of two straight-cut rotors which rotate in the same direction about non-coincident parallel axes [1]. The outer rotor profile forms a conjugate pair with the inner rotor such that there are continuous points of contact between the two during rotation. This allows the separation of the volume between the rotors into multiple working chambers. The volume of each working chamber varies with rotor position, with zero or non-zero minimum volumes possible depending on the choice of rotor geometry. Fixed porting located in the casing of the machine allows control over the periods during which fluid is able to enter and leave these working chambers. Methods of generating the rotor geometry for gerotor applications are described by Colbourne [2], Beard et al [3], Vecchiato et al [4] and Hsieh et al [5,6], and several authors describe numerical approaches to the analysis of gerotor pump performance [1, 7, 8]. Varying the shape of the inlet and/or discharge ports allows the gerotor configuration of positive displacement machine to achieve internal compression or expansion [9], but there is a lack of rigorous investigations of performance for these machines in the literature.

The geometry of helical internally geared rotors based on epi & hypocycloid curves is described by Moineau [10], where varying the helix pitch or profile along the length of the rotor is proposed as a method of achieving internal compression or expansion of the fluid. Adams & Beard [11] considered basic geometrical features of such helical rotors formed from epi & hypotrochoids.

More recently, the concept of conical internally-geared rotors with varying profile and non-parallel axes has been developed for compressor applications [12]. This configuration presents challenges in achieving high accuracy in the manufacture of rotors using efficient and economical methods, and a simpler configuration using constant pitch and profile rotors with stationary porting has been proposed by the authors [13, 14]. For compression applications, these gerotor profiles with helical twist have been shown to reduce the power transfer between rotors [15]. As with conventional twin-screw machines, low power transfer is expected to be an important factor in reducing friction and wear in the rotors, thereby improving durability and limiting the degradation of performance over time.

The gerotor-type screw compressor can be considered as an alternative form of the conventional twin-screw machine. Both configurations have rotors with constant pitch and profile, which rotate about fixed, parallel axes. The gerotor-type machine can be thought of as a conventional machine in which the gate rotor has been wrapped around the main rotor. The present study focuses on important geometrical characteristics of this gerotor-type internally geared screw machine. To understand the potential benefits of this configuration, it is instructive to consider a comparison of the influence of rotor geometry on the relative size of the machines required to deliver the same swept volume. As the performance of the machine is influenced by the pressure drop that occurs across the ports during filling and discharge of the machine, and the leakage of working fluid between working chambers, the port flow areas and the rotor tip leakage line lengths are also characterised as a function of rotor geometry. The key findings of this research have previously been published as an executive summary in the Proceedings of the 11th International Conference on Compressor and Their Systems [16]. A detailed discussion of the analysis and results are presented in the following sections.

2. Geometry of simple rotor profiles for internally geared machines

Gerotor profiles can be generated by defining a curve in the frame of reference of one rotor, and then applying the condition of meshing to identify the conjugate curve in the frame of reference of the other rotor. The result of this process is the creation of conjugate rotor pairs which maintain continuous points of contact. There are many options for defining the initial curve used in this process, allowing significant scope for optimisation of the rotor geometry for particular applications. In this study, the initial curve is chosen to be a cycloid, generated using the pitch circle of one rotor. It can be shown that the conjugate profile for this is also a cycloid generated using the corresponding rotor pitch circle (illustrated in Fig. 1). These profiles have previously been considered for gerotor pump applications by several authors [3, 5, 7, 11]. The profiles generated have one fewer lobe on the inner rotor than the outer rotors, and can conveniently be defined as combinations of epicycloid and hypocycloid curve sections. The equations defining the coordinates of these cycloid sections of the profiles are shown in Equations 1 and 2.

$$\begin{bmatrix} x_e(\theta) \\ y_e(\theta) \end{bmatrix} = \begin{bmatrix} (\rho_b + \rho_e)cos(\theta) - \rho_e cos(\theta(\rho_b/\rho_e + 1)) \\ (\rho_b + \rho_e)sin(\theta) - \rho_e sin(\theta(\rho_b/\rho_e + 1)) \end{bmatrix} \tag{1}$$

$$\begin{bmatrix} x_h(\theta) \\ y_h(\theta) \end{bmatrix} = \begin{bmatrix} (\rho_b - \rho_h)cos(\theta) + \rho_h cos(\theta(\rho_b/\rho_h - 1)) \\ (\rho_b - \rho_h)sin(\theta) - \rho_h sin(\theta(\rho_b/\rho_h - 1)) \end{bmatrix} \tag{2}$$

Details of the method of profile generation have previously been described by the authors [13]. This is summarised in Fig. 1, where the profiles are defined by the radius of the pitch circle, ρ_p, the number of lobes, N, and the radius of the epicycloid generating circle, ρ_e, where $0 \leq \rho_e \leq \rho_p/N$. It is clear from Figure 1 that ρ_e and ρ_h are equal for both the inner and outer rotors, and that the pitch circle radii are related by the gear ratio, $\rho_{p,o}/\rho_{p,i} = N_o/N_i$. A

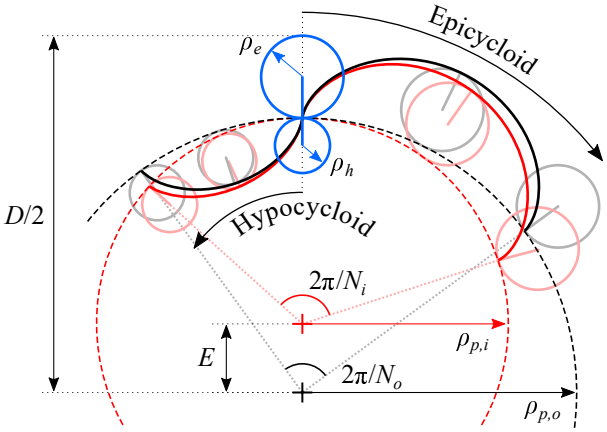

Figure 1: Illustration of the generation of conjugate inner (red) and outer (black) rotor lobe profiles using a combination of epicycloid and hypocycloid curves. Example shown has $N_o = 4$, $N_i = 3$ and $\nu = 0.6$ (hence $\rho_e/\rho_h = 1.5$).

normalised rotor profile parameter, ν, can therefore be defined as follows:

$$\nu = \rho_e/E \quad \text{where } 0 \leq \nu \leq 1 \tag{3}$$

The possible range of values of the profile parameter, $0 \leq \nu \leq 1$, corresponding to the cases when the rotors consist of purely hypocycloid or epicycloid curves respectively. The maximum profile diameter for the outer rotor, D, can be related to the axis spacing, and is found to be a function of ν and the number of lobes on the outer rotor, N_o, as shown in Equation 4.

$$\frac{E}{D} = \frac{1}{2(N_o + 2\nu)} \tag{4}$$

The equation of meshing requires that the normal to both rotor profiles at a contact point must pass through the pitch point of the rotors, and is used to identify the location of the contact points for a given angular position of the rotors. For the composite epi and hypo-cycloid profiles considered here, the loci of contact points between the rotors in the xy plane is found to follow three circular curves corresponding the contact occurring on different sections of the outer and inner profiles, as summarised in Equations 5–7, and illustrated in Figure 2 for the case when $\nu = 0.2$. It is interesting to note that the circular loci with diameters D_e and D_h are exactly the same as the generating circles for the epi and hypo-cycloid curves as shown in Figure 1, meaning that $D_e = 2\rho_e$ and $D_h = 2\rho_h$.

$$\text{Epi-Epi contact:} \quad \frac{D_e}{D} = \nu\frac{E}{D} \tag{5}$$

$$\text{Hypo-Hypo contact:} \quad \frac{D_h}{D} = (1-\nu)\frac{E}{D} \tag{6}$$

$$\text{Hypo-Epi contact:} \quad \frac{D_\ell}{D} = \frac{1}{2} + \frac{E}{D}(N_o - 2) \tag{7}$$

The results in Figure 2 illustrate that as ν increases and more of the rotor is defined by epicycloid curves, the axis spacing E (equal to half the sum of the contact loci diameters D_e and D_h) and the largest contact loci diameter, D_ℓ, are both seen to decrease for rotors of the same outer diameter, D. This is an important point to note, as D_ℓ, D_e and D_h will influence the lengths of the rotor-to-rotor sealing lines that are formed between helical rotors. The trend of

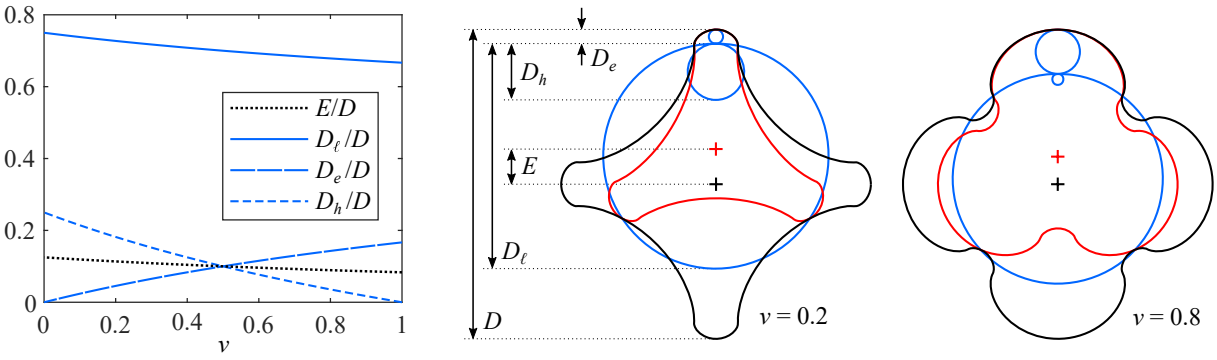

Figure 2: Axis spacing and contact loci paths and diameters (shown in blue) as functions of ν for rotors with $N_o = 4$.

decreasing E/D and D_ℓ/D with increasing ν is seen for all values of N_o, but the effect becomes proportionally smaller as N_o increases and the ratio $N_i/N_o \to 1$. These results suggest that for rotors with the same values of N_o, D, L, and outer rotor wrap angle Φ_o, larger values of ν will achieve shorter helical path lengths for the contact points, and hence shorter sealing lines for the working chamber.

The value of ν also dictates the angular position of the outer rotor at which a working chamber first forms, $\phi_{o,st}$, and at which it ends, $\phi_{o,end}$, as shown in Equation 8.

$$\phi_{o,st} = \frac{\pi}{N_o}(1-\nu), \quad \phi_{o,end} = 2\pi + \frac{\pi}{N_o}(1+\nu) \tag{8}$$

In order to define helical rotors, a wrap angle, Φ, must be specified. This is the angle of rotation of the profile between the two end faces of the rotor. The wrap angles for the outer and inner rotor are related by the gearing ratio such that $\Phi_o/\Phi_i = N_o/N_i$. It is possible to normalise the wrap angle for the outer rotor as shown in Equation 9.

$$\bar{\Phi}_o = \frac{\Phi_o}{\phi_{o,end} - \phi_{o,st}} = \frac{\Phi_o}{2\pi(1+\nu/N_o)} \tag{9}$$

A value of $\bar{\Phi}_o = 1$ corresponds to the case when the maximum volume of a working chamber is achieved at a single position where the cross-sectional area reduces to zero at both end faces; in this case the low pressure end face can be open, as the working chamber is not exposed during compression. If $\bar{\Phi}_o < 1$, the maximum working chamber volume occurs when $A_{wc} > 0$ at both end faces, and low pressure porting is needed is need to ensure that the working chamber is sealed during compression.

Once the geometry of the rotors is defined and the contact points identified, the area of the working chamber contained between two contact points can then be assessed, and by integration of the area along the length of the rotors the working chamber volume can be found [15]. The swept volume created per revolution of the outer rotor, V_{sw}, can then be calculated; this volume can be normalised by the cylindrical volume containing the rotor profiles as shown in Equation 10. A contour plot of $\bar{V}_{sw}$ is shown in Figure 3 as a function of rotor profile parameter, ν, and normalised outer rotor wrap angle, $\bar{\Phi}_o$, for the case when $N_o = 4$. The calculated volume as a function of rotor position can be used to predict the variation in working chamber pressure as discussed in Section 3. Once working chamber pressure is known, the location of contact points can be used to find the net forces and torques acting on the rotors.

$$\bar{V}_{sw} = \frac{V_{sw}}{\pi L D^2/4} = \frac{4N_o \max(V_{wc})}{\pi L D^2} \tag{10}$$

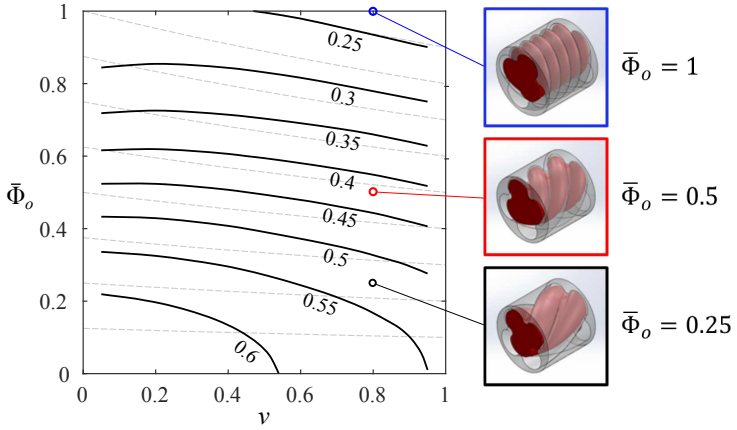

Figure 3: Contour plot of normalised swept volume, $\bar{V}_{sw}$, as a function of profile parameter ν and normalised wrap angle $\bar{\Phi}_o$ for $N_o = 4$; lines of constant wrap angle Φ_o are shown as dashed grey lines.

3. Modelling of the compression process

The internally-geared screw compressor with cycloidal rotor profiles has previously been analysed by the authors using a quasi-1D single chamber model approach to calculate the working chamber pressure and the resulting rotor torques and bearing forces [13, 15]. This simplified analysis is based on the adiabatic compression of an ideal gas, neglecting leakage and pressure losses during filling or discharge, and allows an initial prediction of the pressure variation during the compression process. The net effect of all working chambers on the rotor torque can then be found, and previous analysis [13] has identified a value of $\nu = 0.8$ as suitable to achieve relatively low net torque on the inner rotor when the outer rotor is driven for a range of values of ϵ_v and $\bar{\Phi}_o$ when $N_o = 4$, as shown in Figure 4. This ensures that a high proportion of the power input to the compressor is transferred directly to the fluid, with only a small proportion transferred between the rotors. As with conventional twin-screw compressors, limiting rotor-to-rotor contact forces, and hence rotor wear, is an important requirement due to the need to maintain small clearance gaps for low leakage and high compressor performance.

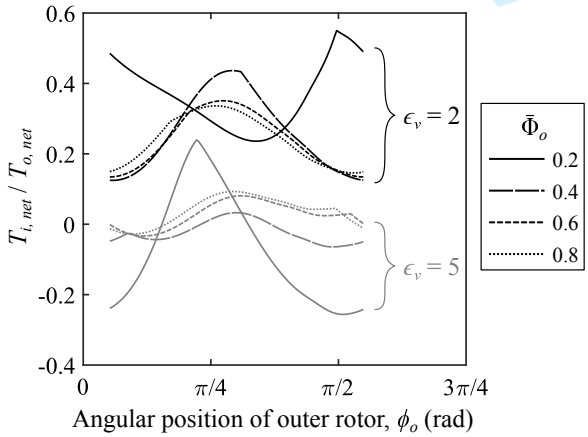

Figure 4: Ratio of net torque on the inner and outer rotors for a single cycle when $N_o = 4$, $\nu = 0.8$, $\bar{\Phi}_o = 0.2, 0.4, 0.6, 0.8$ with $\epsilon_v = 2$ (black lines) and $\epsilon_v = 5$ (grey lines), based on an adiabatic compression cycle with no leakage or port pressure losses as described by Read et al. [13].

4. Geometric properties

Previous studies have investigated the influence of the profile parameter, ν, number of lobes, N_o, and the built-in volume ratio of the compressor, ϵ_v, on the swept volume and driven-to-undriven rotor torque ratio [13, 14]. The aim of this paper is to consider how the port and leakage areas compare between conventional and internally geared screw machines when sized to achieve the same swept volume. This has been achieved by considering a representative conventional screw compressor with N-profile rotors (as illustrated in Figure 5). This machine is a typical design for a small oil-injected air compressor, and the key geometrical parameters are as follows:

- Rotor centre distance = 71.00mm
- Rotor length = 157.97mm
- Main rotor outer diameter = 101.91mm
- Gate rotor outer diameter = 80.17mm
- Main rotor wrap angle = 306°
- Swept volume = 0.720 litres/rev of the main rotor

In order to compare this conventional machine with the proposed internally geared configuration, the case with $N_o = 4$ and $\nu = 0.8$ (as illustrated in Figure 2) was considered, allowing a direct comparison with the conventional machine, as the driven rotor has 4 lobes in both cases. The maximum profile radius for the outer rotor was chosen to be equal to the centre distance in the conventional machine (71mm). An example of this rotor profile is shown in Figure 6b which also shows the high and low pressure port areas calculated for the case when the normalised wrap angle for the outer rotor, $\bar{\Phi}_o = 0.5$, and the built-in volume ratio, $\epsilon_v = 2$.

4.1. Swept volume

The swept volume of the conventional and internally geared configurations can be compared by considering the normalised swept volume, $\bar{V}_{sw}$, which is equal to the swept volume divided by the containing volume of the casing. This is illustrated in Figure 5a. The volume of the conventional machine is seen to remain constant as the wrap angle increased to around 270°. This is because the working chamber cross-sectional area remains constant (between each rotor and the casing) for much of the rotation. In contrast, the internally geared machine has an area that reaches a maximum at only one position; the result is that the swept volume decreases as soon as the wrap angle increases above zero. For wrap angles below around 270° however, the normalised swept volume for the internally geared machine is higher.

A comparison of the conventional and internally-geared screw machines has been made by selecting rotor dimensions that achieve a constant swept volume of 0.720 litres per revolution. As the maximum profile radius of the outer rotor in the gerotor-type configuration has been specified as 71mm, the necessary rotor length therefore depends on the values of both ν and the wrap angle. The resulting L/D ratio as a function of wrap angle of the driven rotor is shown in Figure 6b for the case when $\nu = 0.8$, and these values are used in the following analysis.

4.2. Port areas

In order to investigate the axial port areas that occur with the different configurations, the length of the internally geared rotors must be scaled to achieve the same swept volume. The resulting working chamber volume as a function of rotor position is shown in Figure 6a for the conventional machine and internally geared machines with normalised wrap angles ranging from 0 to 0.9. The corresponding low pressure (LP) and high pressure (HP) axial port flow areas are shown in Figure 6b. These are the areas of the working chamber end faces that are exposed to the port openings during filling and emptying of the working chamber. Figure 6b also shows an example of the rotor geometry and the port areas (external views towards the low and high pressure end-faces of the machine) for the case when $\bar{\Phi}_o = 0.5$.

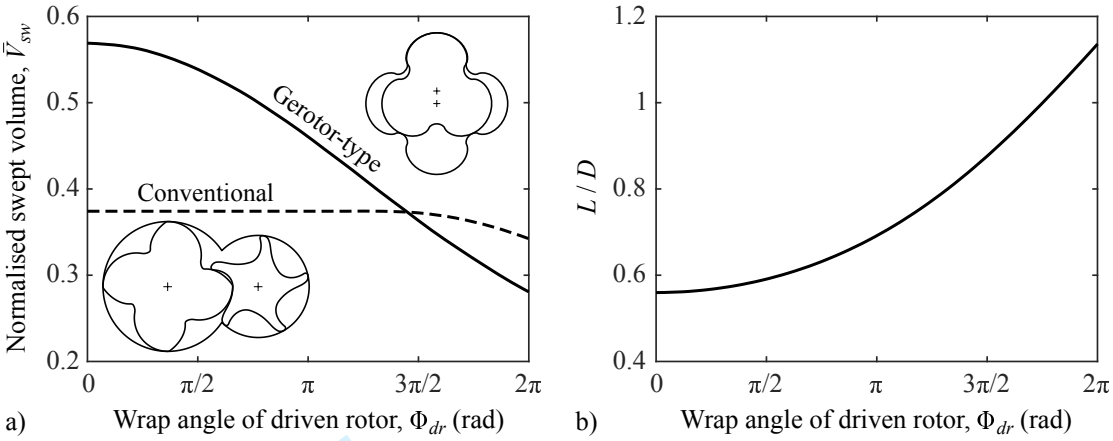

Figure 5: a) Normalised swept volume as a function of the wrap angle of the driven rotor for an internally geared machine with $N_o = 4$ and $\nu = 0.8$ (solid line) and the conventional machine (dashed line), and b) L/D required to achieve constant value of $V_{sw} = 0.720$ litres/rev and with a fixed maximum profile radius = 71mm.

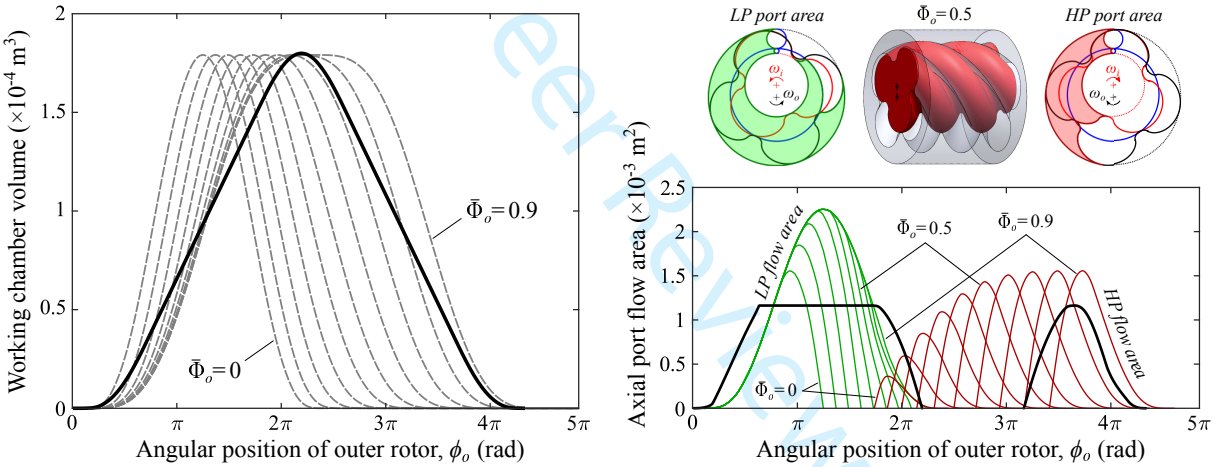

Figure 6: a) working chamber volume and b) port flow areas (with external views of the port geometry shown for $\bar{\Phi}_o = 0.5$) for internally geared machine with $\nu = 0.8$ and $\epsilon_v = 2$ for conventional machine (black line) and gerotor-type machine with $\bar{\Phi}_o = 0 - 0.9$. Note that L/D values for the internally geared machine have been adjusted as shown in Figure 5b to maintain a constant value of V_{sw}.

The results in Figure 6 show that while the maximum working chamber volume is the same in all cases, the maximum rate of change of volume with rotor position, $dV_{wc}/d\phi_o$, reduces with increasing wrap angle for the internally geared machine. It does however remain significantly higher than in the conventional machine. The characteristic port flow area curves also show significant differences between the two types of machine. For all wrap angles, the maximum low pressure area is higher for the internally geared case, while the maximum high pressure port area is higher when $\bar{\Phi}_o > 0.3$.

These results can be compared on the basis of port flow area as a function of $dV_{wc}/d\phi_o$; this is illustrated in Figure 7 for the case when $\bar{\Phi}_o = 0.5$. Although more rigorous chamber modelling is required to understand how the working chamber pressure will vary with volume, the result suggests that, in this case, the port losses will be similar, as the higher rate of volume change is

balanced by the higher maximum flow areas.

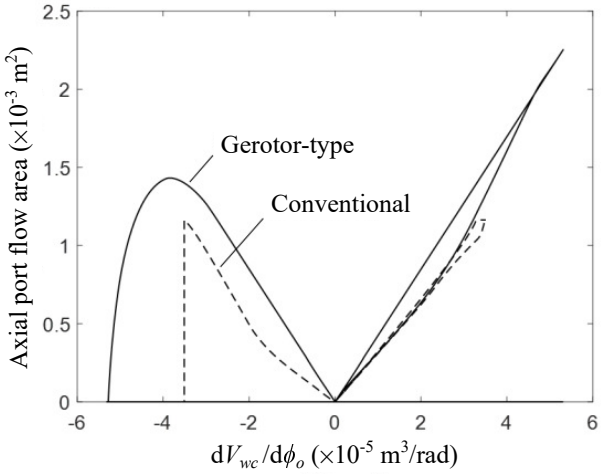

Figure 7: Axial port flow area as a function of the rate of change of working chamber volume with angular position of driven rotor for internally geared gerotor-type machine with $\nu = 0.8$ and $\bar{\Phi}_o = 0.5$ (solid line) and conventional machine (dashed line); $\epsilon_v = 2$ in both cases.

4.3. Leakage line lengths

Another important factor in understanding the performance of these machines is the leakage areas. In the internally geared machines, the length of the leading and trailing edges of the volume contained between the two rotors can be found by considering the coordinates of the contact points throughout the working chamber. This is illustrated in Figure 8, showing the leading and trailing contact points of a particular working chamber in a general cross section through the rotors. For the conventional machine most of the contact at the leading and trailing edges of the working chamber is between the rotors and the casing; although not a leakage path at the working chamber cross-section shown, the 'interlobe' rotor-to-rotor contact point is illustrated as this leakage path exists at some locations within the working chamber and is important due to the high pressure difference present, even though the leakage area is relatively small for most of the cycle (see Figure 9). The gerotor-type machine only ever has rotor-to-rotor contact at the leading and trailing edges of the working chamber. Unlike conventional machines these internally geared machines have no 'blow-hole' leakage area, as the helix on both rotors has the same orientation.

The results for the gerotor-type configuration show that the length of the sealing line for leading and trailing edges are identical and apply to both increasing and decreasing volume due to the symmetric rotor lobe profiles. For the non-symmetrical profile used in the conventional machine there are leading and trailing edges between both rotors and the casing, and an interlobe sealing line (as shown in Figure 8) which vary with working chamber volume, and are different depending on whether the volume is increasing or decreasing. These individual sealing line lengths are shown in Figure 9a for the cases considered in Section 4.2, while the total length of these sealing lines is shown in Figure 9b.

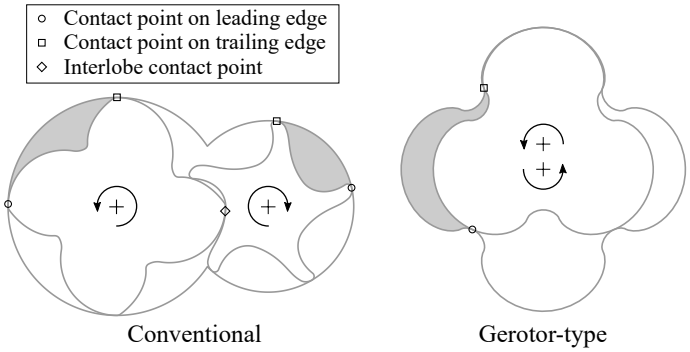

Figure 8: Illustration of contacts points forming the leakage paths at the leading and trailing edges of a working chamber (depicted by shaded areas) in conventional and gerotor-type compressors.

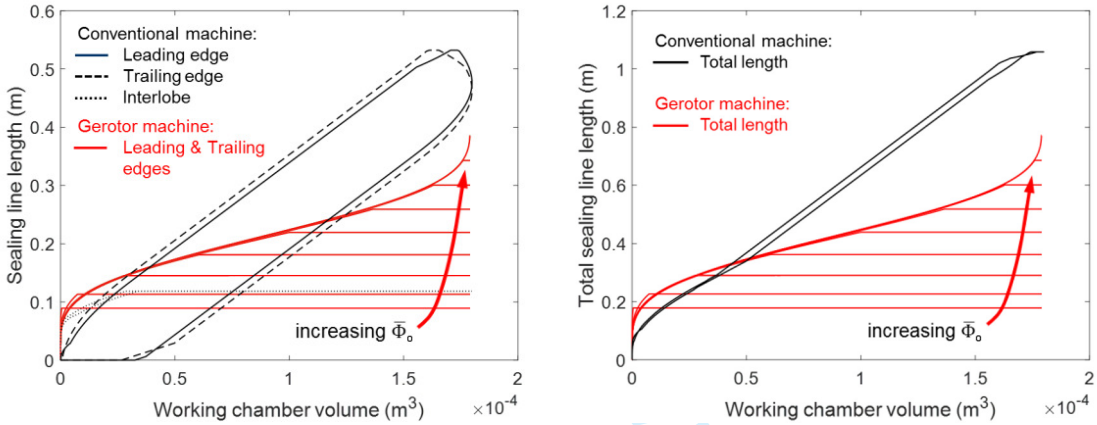

Figure 9: a) individual and b) total sealing line lengths for the conventional machine described in Section 4, and internally geared machines with $\nu = 0.8$ and $\bar{\Phi}_o = 0.1 - 0.9$.

The results in Figure 9 show that the maximum sealing line length increases with the wrap angle for the internally geared machine. For all values of $\bar{\Phi}_o$ it can be seen that the total sealing line length is higher than for the conventional machine at low working chamber volumes, while above a volume of around $0.25V_{wc,max}$ the length is lower in all cases. The overall effect of these leakage line lengths will depend on a range of factors including the manufacturing tolerance of the rotors, the geometry of the leakage paths, the working fluid and the influence of oil injection. It is, however, clear from the results in Figures 6 and 9 that a compromise is necessary between increasing the port flow areas and minimising the inter-rotor leakage areas.

4.4. Influence of profile shape on machine geometry

The choice of rotor profile shape influences both the port shape, the swept volume and the diameter of the rotor contact loci circles. For helical rotors, this will effect the inlet and discharge flow areas, and the length of the rotor-to-rotor contact lines. A comparison has been made using different values of ν with the same fixed value of $D = 142mm$, and adjusting the length of the rotors in order to achieve the same swept volume of the machine.

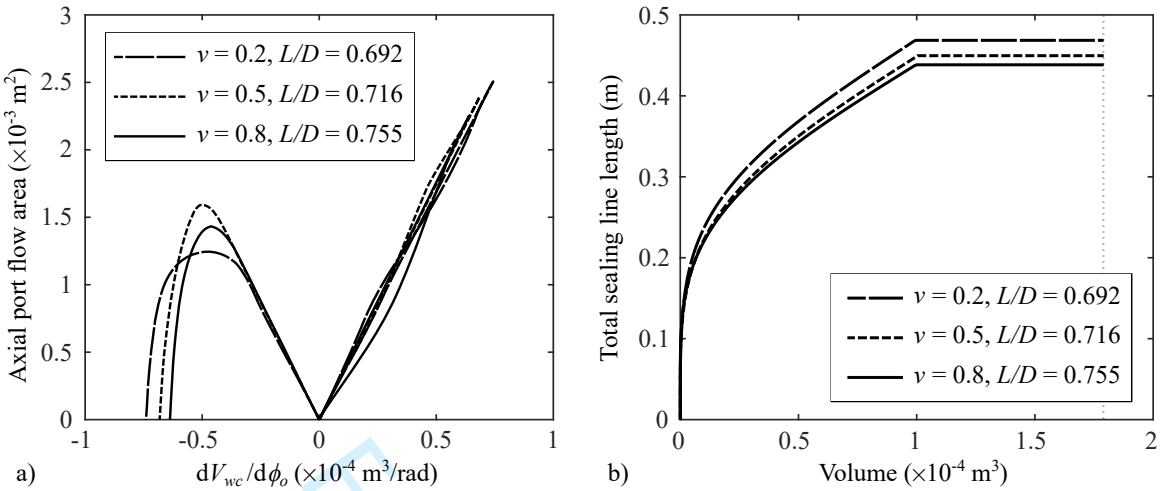

Figure 10: Influence of ν value on a) the axial port flow area as a function of the rate of change of working chamber volume, and b) the total rotor-to-rotor leakage line length; note that $\bar{\Phi}_o = 0.5$, $\epsilon_v = 2$, and the values of D and V_{sw} are the same in all cases.

The results in Figure 10 show that increasing the value of ν increases the maximum rate of change of V_{wc} and has some influence on the high pressure flow area of the machine. The results also show that despite $\bar{V}_{sw}$ increasing with decreasing ν (as shown in Figure 3), and hence a decrease in the required rotor length, the total rotor-to-rotor leakage line length increases due to the larger loci contact path diameter, D_ℓ. These results suggest that a high value of ν may therefore achieve higher efficiency due to reduced leakage losses. Future work will focus on the development of a chamber model to quantify the combined influence of port flow areas and leakage areas on the performance of the internally-geared screw compressor, and identify optimum rotor geometry for specific applications.

5. Conclusions

The influence of the profile, length and wrap angle of rotors on the port and leakage areas in an internally geared gerotor-type compressor have been investigated. The results have been compared with data for a conventional twin-screw oil injected air compressor. The conclusions from the study are as follows:

- When sized for identical enclosed volumes, and using low wrap angles, the internally geared compressor configuration is able to achieve a higher swept volume than conventional screw machines. Increasing the wrap angle causes V_{sw} to decrease more rapidly for the internally geared machine due to the continuous variation of working chamber cross-sectional area along the length of the rotors. This is in contrast to conventional machines, where the working chamber area remains constant through a large range of angular positions, resulting in a constant swept volume from a wrap angle of zero up to around 270°.
- When sized for constant swept volume per revolution of the driven rotor, the maximum value of $dV_{wc}/d\phi_{dr}$ (rate of change of working chamber volume w.r.t. angular position of the driven rotor) is higher for the internally geared configuration (with $N_o = 4$, $\nu = 0.8$ and $0 \leq \bar{\Phi} \leq 0.9$) than for the conventional machine. While this leads to higher port flow rates during filling and discharge of the working chamber, it is balanced to some degree by the maximum axial port flow areas being higher than the conventional machine in all case for the suction port, and when $\bar{\Phi}_o > 0.3$ for the discharge port.

- When sized for constant swept volume per revolution of the driven rotor, the total tip sealing line lengths are found to be lower for the internally geared machine when $V_{wc} > 0.25V_{wc,max}$, with the maximum value increasing with increasing wrap angle.
- For the internally geared configuration with fixed values of $\bar{\Phi}_o$, maximum profile diameter and swept volume, decreasing the value of ν is seen to increase both the maximum rate of change of volume during discharge and the maximum total sealing line length. This suggests that machines with a higher value of ν are likely to have lower porting and leakage losses, and a higher overall efficiency.

It is important to note that these findings are based only on the geometrical characteristics of gerotor-type screw machines using cycloidal rotor profiles. The efficiency of these machines will depend on a range of factors including the geometry of rotors and their manufacturing tolerances, the geometry of the leakage paths, the working fluid, and the required suction and discharge pressures and mass flow rate. The focus of future work will be to apply the port and sealing line geometry discussed in this paper in a detailed thermodynamic multi-chamber model to characterise the influence of leakage and port losses on compressor performance. The model will allow the optimisation of key geometrical parameters including rotor profiles, lobe number, wrap angle, and L/D ratio in order to maximise the specific power of the machine for a range of applications. This is expected to provide a rigorous basis for comparison with twin-screw and other positive displacement compressors, and determine the viability of the internally geared configuration.

Nomenclature

A	Area (m^2)
D	Maximum profile diameter (m)
$D_{e,h,\ell}$	Diameter of rotor contact loci circles (m)
E	Distance between rotor axes (m)
L	Rotor length (m)
N	Number of lobes on rotor
T	Rotor torque (Nm)
V	Volume (m^3)
V_{sw}	Swept volume (m^3/rev)
ρ	Radius (m)
ν	Cycloid rotor profile parameter (-)
θ	Cycloid generating angle (rad)
ϕ	Rotor angular position (rad)
Φ	Wrap angle of rotor (rad)
ϵ_v	Built-in volume ratio

Subscripts

wc	Relating to a working chamber
i, o	Inner or outer rotor
e, h	Epi or hypo cycloid
p	Pitch circle for cycloid generation

References

[1] Rundo, M., 2017. Models for flow rate simulation in gear pumps: A Review. Energies, 10(9), p.1261.
[2] Colbourne, J.R., 1974. The geometry of trochoid envelopes and their application in rotary pumps. Mechanism and Machine Theory, 9(3-4), pp.421-435.

[3] Beard, J.E., Yannitell, D.W. and Pennock, G.R., 1992. The effects of the generating pin size and placement on the curvature and displacement of epitrochoidal gerotors. Mechanism and Machine Theory, 27(4), pp.373-389.
[4] Vecchiato, D., Demenego, A., Argyris, J. and Litvin, F.L., 2001. Geometry of a cycloidal pump. Computer methods in applied mechanics and engineering, 190(18), pp.2309-2330.
[5] Hsieh, C.F. and Hwang, Y.W., 2007. Geometric design for a gerotor pump with high area efficiency. Journal of Mechanical Design, 129(12), pp.1269-1277.
[6] Hsieh, C.F., 2009. Influence of gerotor performance in varied geometrical design parameters. Journal of Mechanical Design, 131(12), p.121008.
[7] Hsieh, C.F., 2012. Fluid and dynamics analyses of a gerotor pump using various span angle designs. Journal of Mechanical Design, 134(12), p.121003.
[8] Gamez-Montero, P.J., Castilla, R., Mujal, R., Khamashta, M. and Codina, E., 2009. GEROLAB package system: Innovative tool to design a trochoidal-gear pump. Journal of Mechanical Design, 131(7), p.074502.
[9] Mathias, J.A., Johnston, J.R., Cao, J., Priedeman, D.K. and Christensen, R.N., 2009. Experimental testing of gerotor and scroll expanders used in, and energetic and exergetic modeling of, an organic Rankine cycle. Journal of Energy Resources Technology, 131(1), p.012201
[10] Moineau, R.J.L., 1932. Gear mechanism. U.S. Patent 1,892,217.
[11] Adams, G.P. and Beard, J.E., 1997. Comparison of helical and skewed axis gerotor pumps. Mechanism and Machine Theory, 32(6), pp.729-742.
[12] Dmitriev, O. and Arbon, I.M., 2017, August. Comparison of energy-efficiency and size of portable oil-free screw and scroll compressors. In IOP Conference Series: Materials Science and Engineering (Vol. 232, No. 1, p. 012057). IOP Publishing.
[13] Read M.G., Smith I.K., Stosic N., 2017. Internally geared screw machines with ported end plates. In IOP Conference Series: Materials Science and Engineering 2017 Aug (Vol. 232, No. 1, p. 012058). IOP Publishing.
[14] Read M.G., Smith I.K., Stosic N., 2017. Operational characteristics of internally geared positive displacement screw machines. In International Mechanical Engineering Congress and Exposition 2017 Nov 3 (pp. V006T08A032-V006T08A032). American Society of Mechanical Engineers.
[15] Read, M.G., Stosic, N. and Smith, I.K., 2019. The influence of rotor geometry on power transfer between rotors in gerotor-type screw compressors. ASME Journal of Mechanical Design, 142(7): 073501.
[16] Read, M.G., Smith, I.K. and Stosic, N., 2019. Geometrical Comparison of Conventional and Gerotor-Type Positive Displacement Screw Machines. In IOP Conference Series: Materials Science and Engineering (Vol. 604, No. 1, p. 1).

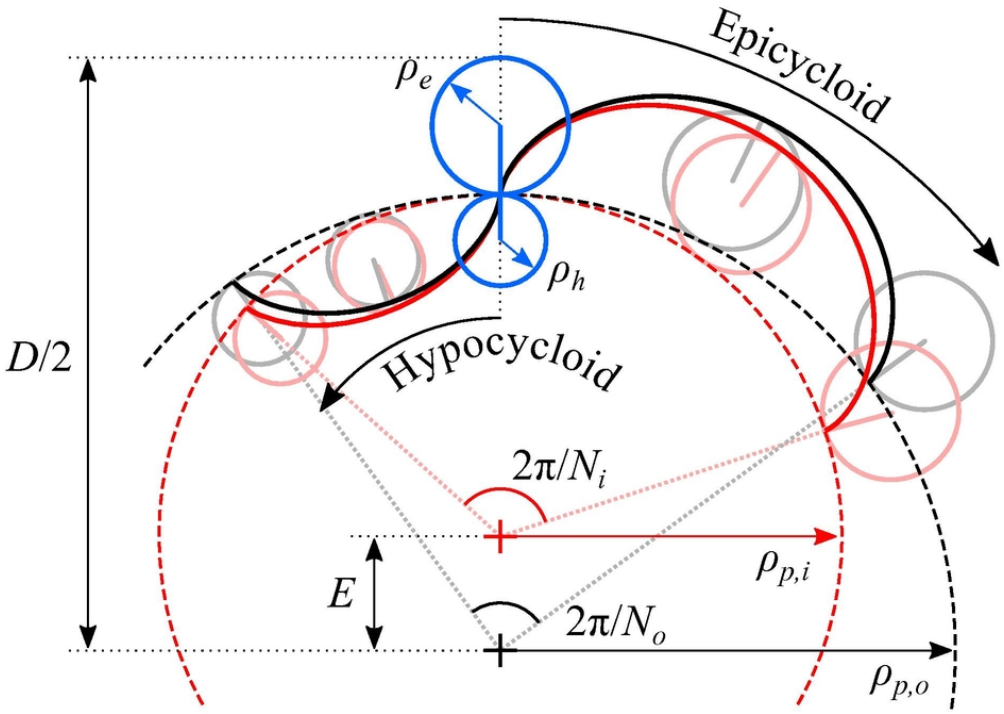

Illustration of the generation of conjugate inner (red) and outer (black) rotor lobe profiles using a combination of epicycloid and hypocycloid curves. Example shown has $N_{o}=4$, $N_{i}=3$ and $nu=0.6$ (hence $rho_e/ rho_h=1.5$).

79x56mm (300 x 300 DPI)

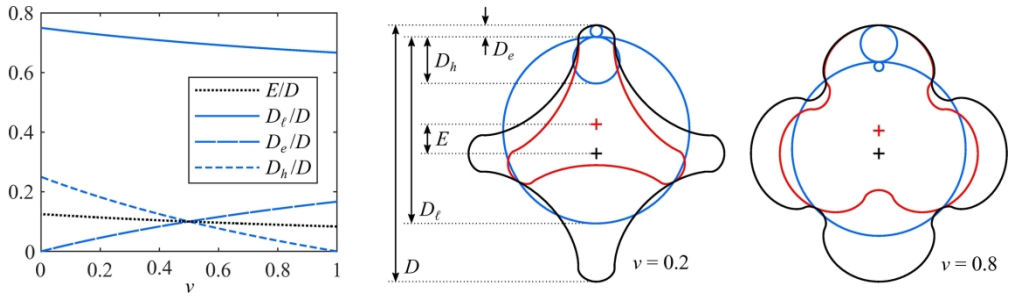

Axis spacing and contact loci paths and diameters (shown in blue) as functions of nu for rotors with $N_{o}=4$.

205x58mm (300 x 300 DPI)

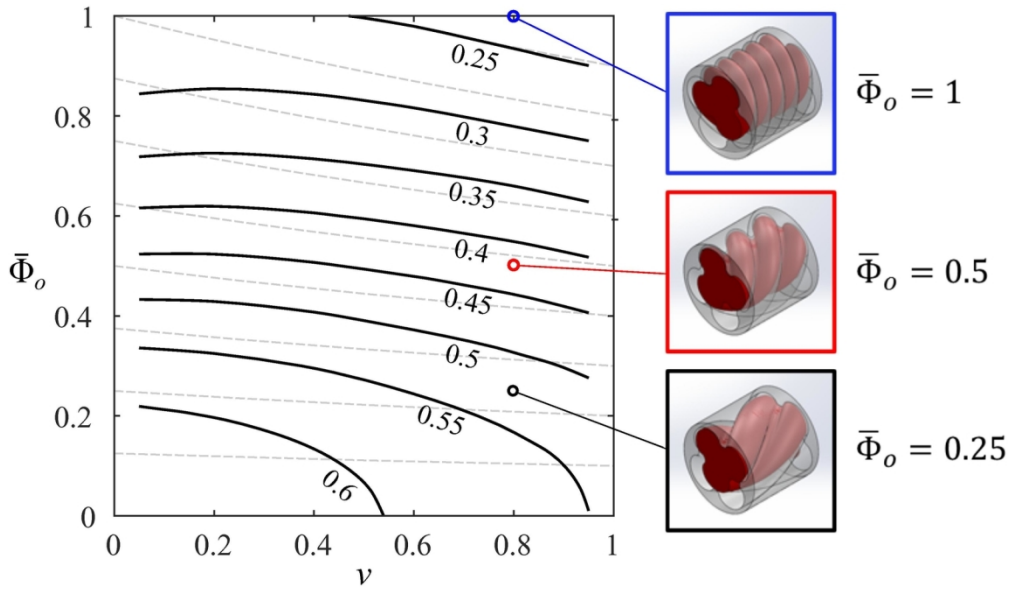

Contour plot of normalised swept volume, $\bar{V}_{sw}$, as a function of profile parameter nu and normalised wrap angle $\bar{\Phi}_{o}$ for $N_{o}=4$; lines of constant wrap angle Φ_{o} are shown as dashed grey lines.

139x81mm (300 x 300 DPI)

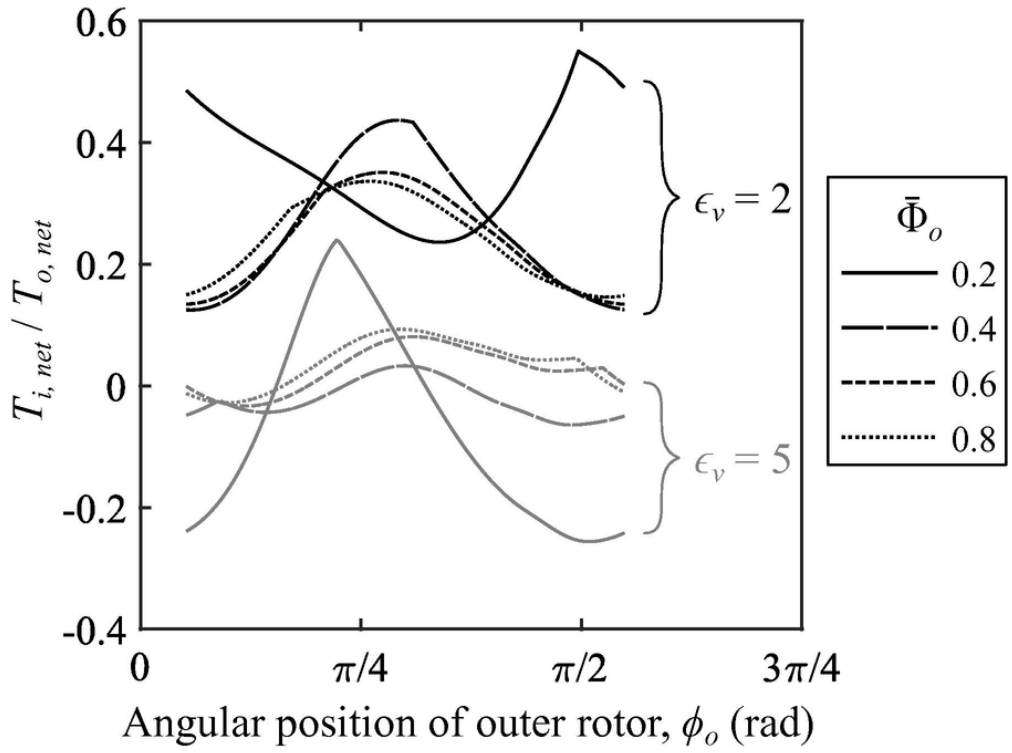

Ratio of net torque on the inner and outer rotors for a single cycle when $N_{o}=4$, $ u=0.8$, $\bar{\Phi}_{o}=0.2,0.4,0.6,0.8$ with $\epsilon_{v}=2$ (black lines) and $\epsilon_{v}=5$ (grey lines), based on an adiabatic compression cycle with no leakage or port pressure losses as described by Read et al. [13].

76x57mm (300 x 300 DPI)

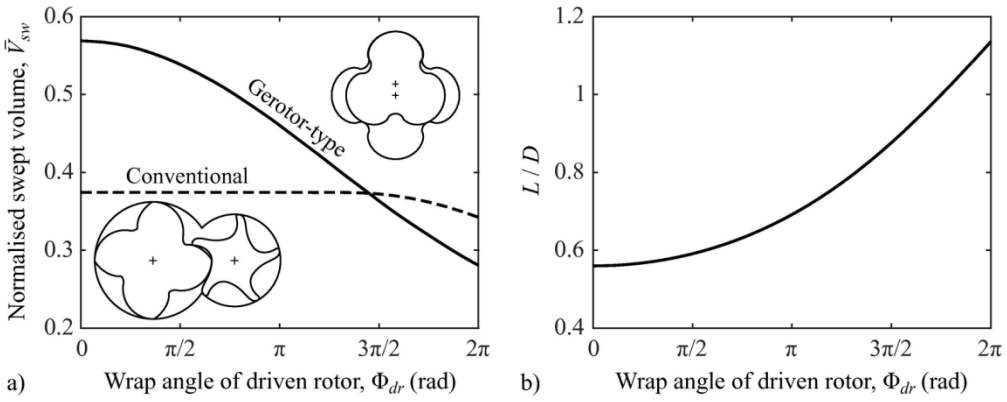

a) Normalised swept volume as a function of the wrap angle of the driven rotor for an internally geared machine with $N_{o}=4$ and $nu=0.8$ (solid line) and the conventional machine (dashed line), and b) L/D required to achieve constant value of $V_{sw}=0.720 litres/rev$ and with a fixed maximum profile radius = 71mm.

146x57mm (300 x 300 DPI)

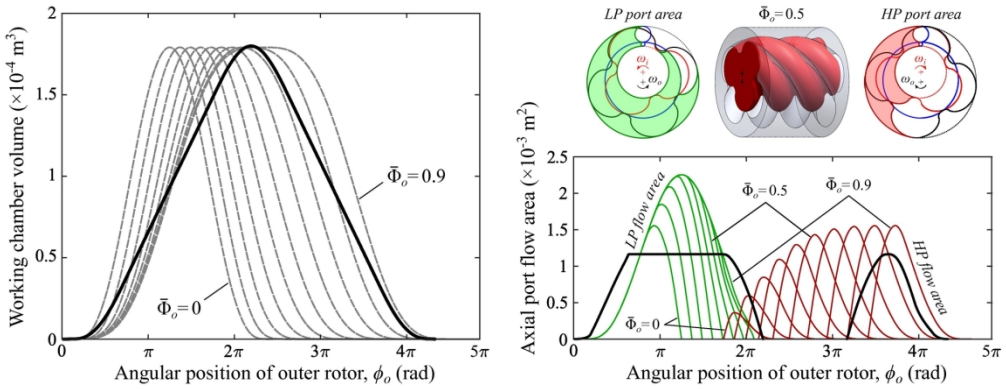

a) working chamber volume and b) port flow areas (with external views of the port geometry shown for $\bar{\Phi}_{o}=0.5$) for internally geared machine with $\nu=0.8$ and $\epsilon_{v}=2$ for conventional machine (black line) and gerotor-type machine with $\bar{\Phi}_{o}=0-0.9$. Note that L/D values for the internally geared machine have been adjusted as shown in Figure \ref{fig_vbar}b to maintain a constant value of V_{sw}.

173x66mm (300 x 300 DPI)

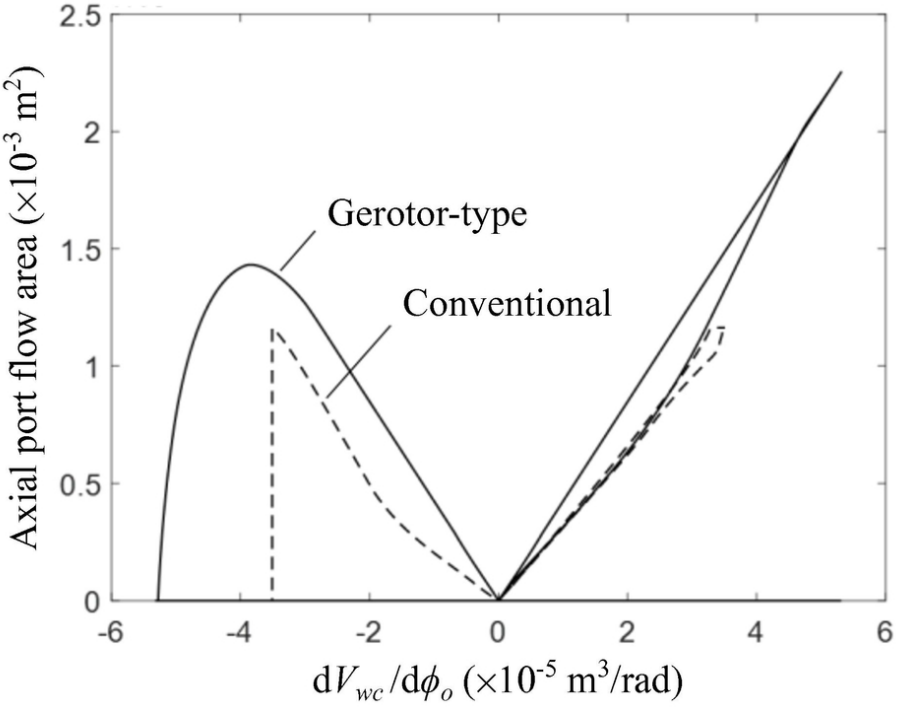

Axial port flow area as a function of the rate of change of working chamber volume with angular position of driven rotor for internally geared gerotor-type machine with $nu=0.8$ and $\bar{\Phi}_{o}=0.5$ (solid line) and conventional machine (dashed line); $\epsilon_{v}=2$ in both cases.

86x64mm (300 x 300 DPI)

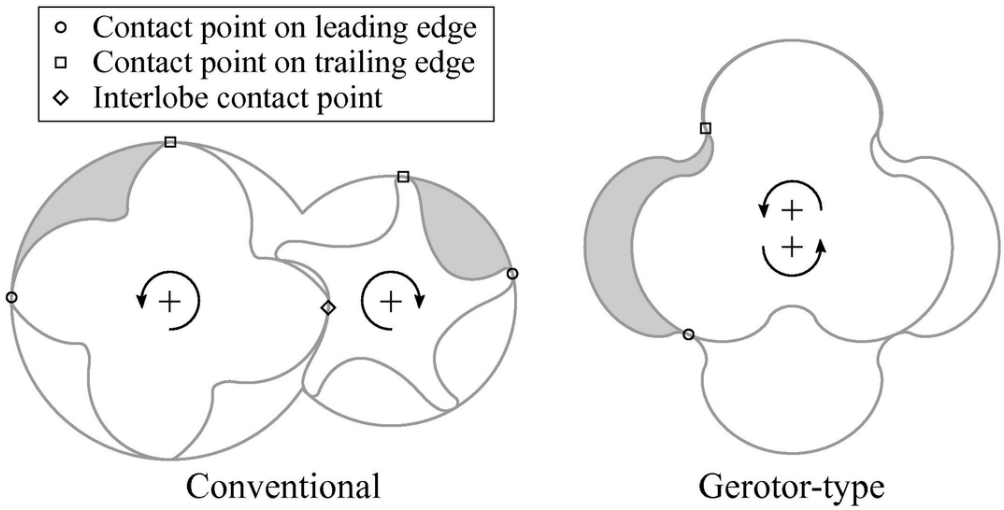

Illustration of contacts points forming the leakage paths at the leading and trailing edges of a working chamber (depicted by shaded areas) in conventional and gerotor-type compressors.

90x45mm (300 x 300 DPI)

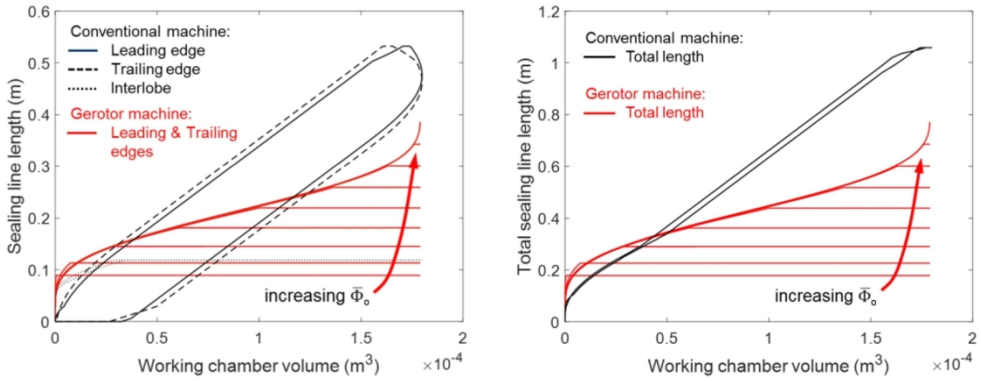

a) individual and b) total sealing line lengths for the conventional machine described in Section 4, and internally geared machines with $nu=0.8$ and $\bar{\Phi}_{o}=0.1-0.9$.

148x58mm (300 x 300 DPI)

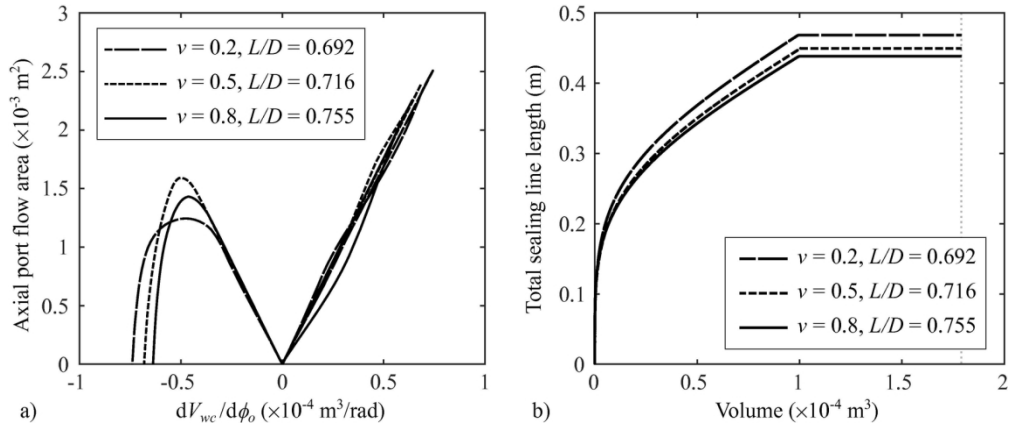

Influence of nu value on a) the axial port flow area as a function of the rate of change of working chamber volume, and b) the total rotor-to-rotor leakage line length; note that $\bar{\Phi}_{o}=0.5$, $\epsilon_{v}=2$, and the values of D and V_{sw} are the same in all cases.

152x63mm (300 x 300 DPI)